

NUMERICAL MODELING OF ION PRODUCTION IN ECRIS BY USING THE PARTICLE-IN-CELL METHOD

V. Mironov, J.P.M. Beijers

Kernfysisch Versneller Instituut, University of Groningen, The Netherlands

Abstract

To better understand the physical processes in ECRIS plasmas, we developed a Particle-in-Cell Monte-Carlo Collisions code that simulates the ionization and diffusion dynamics. The ion production is modelled assuming that the ions are confined by a ponderomotive barrier formed at the boundary of the ECR zone. The main features of ECRIS performance are reproduced, such as the saturation and decrease of highest charge state currents with increasing gas pressure, as well as response to an increase of injected RF power.

INTRODUCTION

The ponderomotive force plays an important role in the ECRIS plasmas [1]. Electrons are partially expelled by a gradient of the microwave electric field from a thin layer around the ECR zone, giving rise to a positive potential that confines the ions. The height of this ponderomotive barrier (PB) is difficult to estimate: it depends on the power density of the microwave radiation, on the gradient of the magnetic field at the resonance, on the plasma density and other factors. Taking the PB height as a free parameter in our calculations, we suppose that it goes to zero when the plasma density approaches the cut-off value because of reflections of the microwaves from the ECR zone boundary and absorption in the plasma.

The ECRIS plasma potential is experimentally known to be positive and around 20-50 V. Roughly half of the potential drop from the plasma to the walls occurs in a thin sheath area (extending a few Debye lengths from the walls), the remaining drop is in a pre-sheath further inside the plasma. The extension of the pre-sheath is unknown, but we here assume that it is located between the ECR zone and the wall sheath. Then, neglecting the PB width, the PB mimics the potential dip, often assumed to be a reason for ion confinement in ECRIS.

The PB confinement of the plasma is accompanied with the gas-dynamics confinement, where the ion pressure gradients govern the rate of ion diffusion to the walls and to the extraction area [2]. The length of the ion production volume defines the ion confinement times, which were found to be linear proportional to the ion charge state [2]. Here we present numerical simulations of the ECRIS plasma combining both confinement models.

CODE DESCRIPTION

The main features of our PIC-MCC code have been described elsewhere [2]. The calculations were done for neon as a feeding gas; the magnetic field and geometry of the source are those of the KVI-AECRIS [3]. The magnetic fields were calculated with POISSON-

SUPERFISH, the hexapole component was calculated analytically, neglecting edge effects.

The elastic ion-ion collisions are modelled using the energy-and-momentum conserving Takizuka-Abe scheme [4], the rates of charge-transfer collisions and elastic collisions between ions and neon atoms are adopted from [5] with linear scaling of the rates as a function of the ion charge state (Z). The charge-transfer reactions for the multiply charged ions result in Coulomb repulsion of the colliding particles and we estimate the Q -value of these reactions to be 10 eV independent of the charge state. Then, even if the rates are relatively small ($\sim 3 \times 10^{-10} \times Z \text{ cm}^3/\text{sec}$) compared to the ionization and ion loss rates, and the neutral density in the chamber is much smaller than the plasma density, the influence of these collisions on the plasma behaviour is not negligible.

Heating due to electron-ion collisions is modeled by kicking the ions at each computational step in a random direction with the velocity diffusion coefficient corresponding to an electron temperature T_e of 1 keV. The ionization rates are calculated according to [6]. The recombination processes can be neglected in our conditions because of their low rates for this T_e .

The static electric field inside the ECR zone is set to zero, and arbitrary set to 1 V/cm along the magnetic field lines outside the zone. The pre-sheath electric field can be varied in a wide range without changing the computational results, as long as there is no backward influence of the pre-sheath area on the main production volume, but the ions are just moving toward the chamber walls and into the extraction aperture.

When hitting the walls, the ions are neutralized and scattered back with an angular distribution according to the cosine-law and with a Gaussian distribution of energies (FWHM=10 eV, peak energy of $10 \times Z$ eV [7]). In collisions with the walls, the neutralized particles lose their energy with a thermal accommodation coefficient taken from [8] for Ne on an Al surface. For initial energies above a few eV, this coefficient is relatively high (~ 0.5) while it goes to almost zero for energies in the meV range. The result is that the kinetic energies of the neutral atoms inside the source chamber are quite high (~ 0.25 eV) and are in the same range as the ion temperatures in the plasma.

When a computational macro-particle hits the extraction aperture (of 0.8 cm diameter), it is injected back into the volume from the injection side with an energy taken from a Maxwell-Boltzmann distribution at room temperature. The total number of computational macro-particles is conserved. Calculations are done until a steady state is reached. Transient processes are not properly calculated in such a scheme. In equilibrium, the

ion flux that goes to the extraction is nearly equal to the gas flow into the chamber, because the ion flux is much higher than the neutral losses to extraction in most cases (ion-pumping effect).

When an ion crosses the ECR resonance surface, its velocity along the magnetic field line is calculated. If the velocity is smaller than a certain value (scaled as \sqrt{Z}), the ion is reflected back to the ECR zone, if not, it is accelerated by the pre-sheath electric field and goes to the walls/extraction. In our model, there are no spatial variations of the height of the PB, and the PB dependence on the plasma density is a step-like function. When the maximal electron density exceeds the limit of $2.5 \times 10^{12} \text{ cm}^{-3}$ (cut-off plasma density for 14 GHz microwaves), the PB value is set to zero, and otherwise it is an input parameter that is varied from 0 to 1 V in our calculations. If the PB value is set to zero, plasma decays and the plasma density falls below the cut-off; after that, ion accumulation begins again. Another way to ensure the saturation of plasma density is an introduction of anomalous ion heating above the cut-off, and it was shown in our calculations that the outputs of both approaches are basically the same.

RESULTS

The positions where the ions hit the extraction/injection plates of the source form the characteristic three-arm stars. The localization of HCI on axis is observed as a result of the ion-ion collisions and the radial gradients of ion densities – the well known effect of the inward transport of the highest charge states. The higher the neutral/ion temperatures, the more pronounced this localization is. The hollow profiles of the ion beams at the extraction were observed when setting the thermal accommodation coefficient to a high value with relatively small ponderomotive barriers.

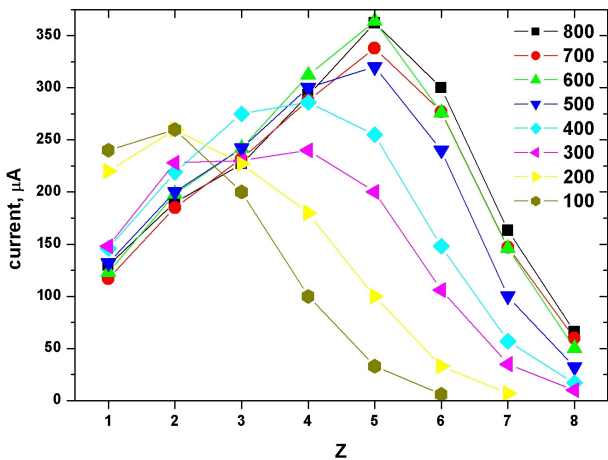


Figure 1: Experimentally observed spectra of extracted neon ions for different RF powers.

The experimental spectra of neon ions extracted from KVI-AECRIS are shown in Fig. 1 as a function of the injected RF power for comparison with simulation results.

The gas flow into the source was fixed at the optimal level for Ne^{6+} production. The total ion flux into the extraction zone is nearly constant ($\sim 500 \mu\text{A}$) for all spectra. Saturation of the source output is observed at RF powers above 800 W.

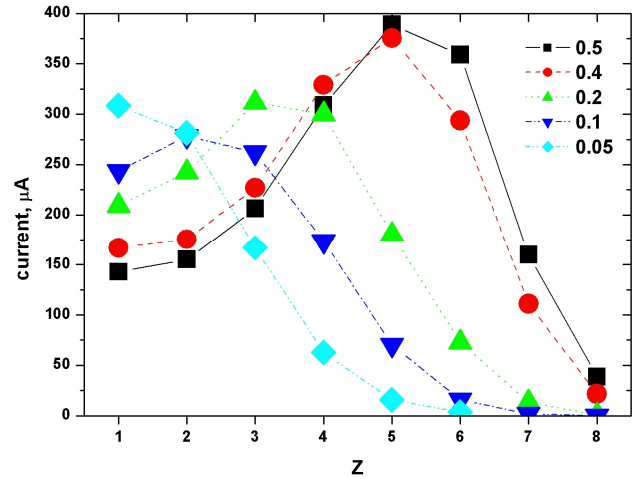


Figure 2: Simulated spectra of extracted neon ions for different ponderomotive barrier values.

The simulated spectra of extracted currents are shown in Fig. 2 for different values of the ponderomotive barrier indicated in the graph. The gas pressure in the chamber was varied for each PB by changing the statistical weight of the computational particles to keep the total flux of ions to the extraction aperture close to $500 \mu\text{A}$. The general experimentally observed features are well reproduced and we observe a linear correspondence between injected RF power and the PB height.

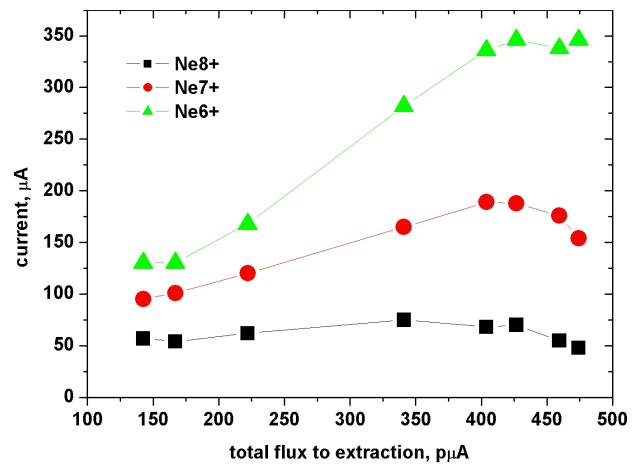


Figure 3: Experimental dependence of the extracted neon currents on the total flux of ions into the extraction (gas flow into the chamber).

In Fig. 3, the measured extracted ion currents of Ne^{6+-8+} are shown as a function of the total extracted ion current. The spectra were measured for an injected RF power of 800 W. The typical saturation of the currents of highly charged ions with increasing total flux is visible, followed

by a drop at still higher total output. Also, the lower the lower the total extracted ion flux, the higher is the mean charge state. For gas flows above the value that corresponds to 500 μA total output current, mode jumps in the source performance were observed that make it difficult to compare the extracted currents with the spectra at the lower pressures.

The simulated dependencies are shown in Fig. 4. The PB height was set at 0.5 V, and the gas pressure was varied by changing the statistical weight of the computational particles.

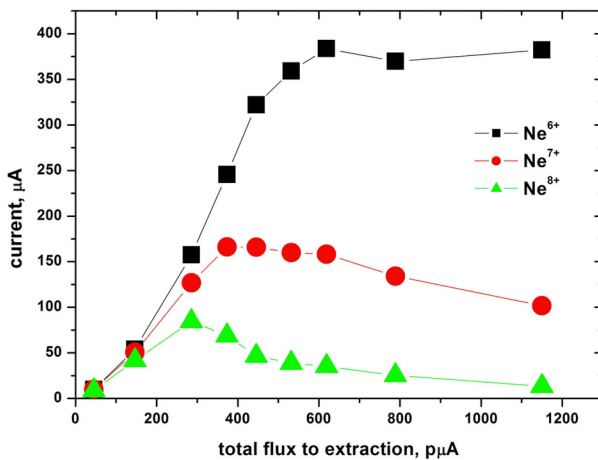


Figure 4: Simulated dependence of the extracted neon currents on the total flux of ions into the extraction (gas flow into the chamber).

It is seen that the currents of Ne^{6+-8+} ions saturate at gas flows that are close to the experimentally observed ones. Though some deviations are seen, the general behavior is well reproduced.

The gas mixing effect was modeled by running simulations with equal numbers of Ne and He macroparticles in the plasma chamber. The currents of neon ions were not observed to be substantially higher in a comparison with no gas-mixing. Ion current saturation and drop occurred at lower gas flows. When switching off Ne-He ion collisions, thus prohibiting thermalization between ions of different elements, the He^{2+} current almost doubled in agreement with the well-known performance degradation when heavier elements are present in the source volume.

Ion confinement times increase with increasing PB height and lower gas flows. The typical dependence of the confinement times as a function of the ion charge state is shown in Fig. 5 for PB=0.5 V and total ion fluxes as indicated in the graph. Ion confinement times are taken as the time difference between the moment of Ne^{1+} creation and the moment when the Ne^{Z+} ion is extracted [2].

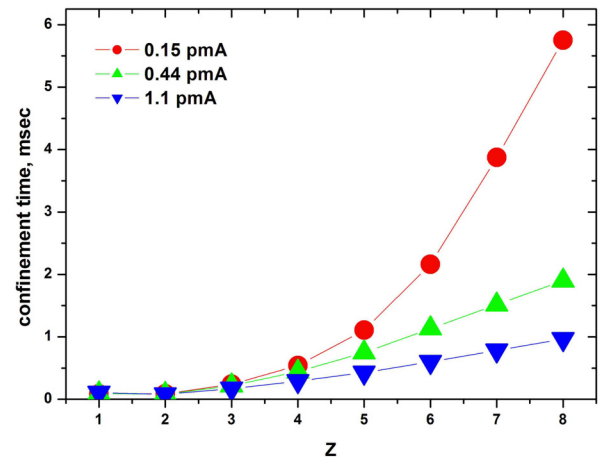


Figure 5: Simulated dependence of the ion confinement times on the ion charge state for different ion fluxes.

For the highest charge states, the dependencies are nearly linear in accordance with the measurements [9].

ACKNOWLEDGMENTS

This work is part of the research program of the “Stichting voor Fundamenteel Onderzoek der Materie” (FOM) with financial support from the “Nederlandse organisatie voor Wetenschappelijk Onderzoek” (NWO). It is supported by the University of Groningen and by the “Gesellschaft für Schwerionenforschung GmbH” (GSI), Darmstadt, Germany.

REFERENCES

- [1] R. Geller, Electron Cyclotron Resonance Ion Sources and ECR Plasma (Bristol: Institute of Physics), 1996.
- [2] V. Mironov and J. P. M. Beijers, Phys. Rev. ST Accel. Beams 12, 073501 (2009).
- [3] H.R. Kremers, J.P.M. Beijers, and S. Brandenburg, Rev.Sci.Instrum. 77, 03A311 (2006).
- [4] T. Takizuka and H. Abe, J.Comp.Phys. 25, 205 (1977).
- [5] D. Piscitelli, A.V. Phelps, J. de Urquijo, E. Basurto, and L.C. Pitchford, Phys.Rev.E 68, 046408 (2003).
- [6] P. Mazzotta, G. Mazzitelli, S. Colfrancesco, N. Vittorio, Astron. Astrophys., Suppl. Ser., 133, 403 (1998).
- [7] J.W. Cuthbertson, W.D. Langer and R.W. Motley, J.Nucl.Mater. 196-198, 113 (1992).
- [8] F.O. Goodman and H.Y. Wachman, J.Chem.Phys. 46, 2376 (1967).
- [9] G. Douysset, H. Khodja, A. Girard and J.P. Briand, Phys.Rev.E 61, 3015 (2000).